Mirror and cavity formations by chains of collectively radiating atoms

Qurrat-ul-Ain Gulfam*
Department of Physics, Faculty of Science, Jazan University, P.O. Box 114, Gizan 45142, Saudi Arabia

Zbigniew Ficek†
The National Centre for Applied Physics, KACST, P.O. Box 6086, Riyadh 11442, Saudi Arabia
and Quantum Optics and Engineering Division, Institute of Physics, University of Zielona Góra, Szafrana 4a, 65-516 Zielona Góra, Poland
(Received 7 July 2016; published 16 November 2016)

We search for mirror and cavitylike features of a linear chain of atoms in which one of the atoms is specially chosen as a probe atom that is initially prepared in its excited state or is continuously driven by a laser field. Short chains are considered, composed of only three and five atoms. The analysis demonstrates the importance of the interatomic dipole-dipole interaction, which may lead to a collective ordering of the emission along some specific directions. We examine the conditions under which the radiative modes available for the emission are only those contained inside a cone centered about the interatomic axis. Particular interest is in achieving one-way emission along the interatomic axis, in either the left (backward) or the right (forward) direction, which is referred to as a mirrorlike behavior of the atomic chain. A direction-dependent quantity called the directivity function, which determines how effective the system is in concentrating the radiation in a given direction, is introduced. We show that the function depends crucially on the distance between the atoms and find that there is a threshold for the interatomic distances above which a strongly directional emission can be achieved. The one-sided emission as a manifestation of the mirrorlike behavior and a highly focused emission along the interatomic axis as a characteristic of a single-mode cavity are demonstrated to occur in the stationary field. Below the threshold the directivity function is spherically symmetric. However, we find that the population can be trapped in one of the atoms, and sometimes in all atoms, indicating that at these short distances the system decays to a state for which there are no radiative modes available for emission.

DOI: 10.1103/PhysRevA.94.053831

I. INTRODUCTION

Advancement in the current technology of trapping and controlling single atoms cooled down to ultralow temperatures has opened new research directions in quantum optics and quantum communication. Spatial configurations of linear atomic chains or two-dimensional atomic lattices have been engineered and have been widely applied in various experimental setups [1–5]. Recently, the subject of utilizing supercold atoms as highly reflecting mirrors has gained much attention. In particular, it has been demonstrated that a collection of cold atoms trapped near the surface of a one-dimensional waveguide can form a nearly perfect mirror for the radiation incident on the atoms [6–8]. The waveguide represents a photonic channel which enhances the electromagnetic field to which the atoms are coupled, thereby leading to a strong collective behavior of the atoms [9]. As a consequence, a large part of the incident light is directed, reflected back, to the medium from which it originated. This striking mirror property of atoms is in contrast to the usual observation, where atoms absorb or scatter all or most of the incident energy.

Another kind of system that can exhibit mirror properties or, equivalently, highly directive radiative properties are atoms chirally coupled to a waveguide [10–12]. Chirality in atom-waveguide coupling is an effect associated with a broken symmetry of emission of photons from the atoms into the right- and left-propagating modes of the waveguide. As a result, the emitted photons are channeled into one of the two directions of the waveguide. It has been shown that the chiral property of the emission can enhance entanglement between two distant atoms [13]. Directive radiative properties have also been demonstrated for a single atom trapped in front of a distant dielectric mirror [14]. It has been demonstrated both theoretically and experimentally that the atom can behave as an optical mirror effectively forming, together with the dielectric mirror, a Fabry-Pérot cavity. Related studies have shown that an atom mirror not only can serve as a single mirror for a one-dimensional cavity, but also can be arranged to behave like a high-finesse cavity [15,16].

In the course of previous work on directional emission the underlying atoms independently couple to a one-dimensional field of a waveguide, or nanocavity, or nanofiber. Although systems involving independent atoms exhibit interesting directional properties, there can be similar features created by an open system of atoms in which the atoms are coupled to a common three-dimensional field. It was Dicke [17] who pointed out that a collection of a large number of atoms coupled to a common electromagnetic field can radiate collectively such that the spontaneous radiation can be enhanced in certain directions. Since then there have been many studies of the collective radiative properties of multiatom systems demonstrating the dependence of the emitted radiation on the number of atoms and the geometry of the emitting system [18–30].

In this paper, we investigate the radiative properties of an open system of a line of a few atoms and demonstrate that the dipole-dipole interaction between atoms may lead to a collective ordering of the emission along some specific directions.

*qgulfam@jazanu.edu.sa
†zficek@kacst.edu.sa

To determine the directions of the emission, we introduce the directivity function of the emitted radiation field and study the dependence of the function on the distance between atoms. We consider directions which lie on a surface perpendicular to the direction of the atomic dipole moments, the horizontal pattern of the radiation field, and analyze the directional properties of the emitted field for two configurations of the atomic chains, one mimicking an atom in front of a mirror and the other an atom inside a cavity. In the first, we choose the left-hand-side atom in the chain as a probe atom and examine conditions under which the system may radiate only to those modes whose propagation vectors lie within a small solid angle about the interatomic axis and oriented in one of the two directions of the interatomic axis, either the right (forward) or the left (backward) direction. Such a system can be regarded as an atom in front of a perfectly reflecting or perfectly transmitting atomic mirror. In the second physical arrangement, we choose the middle atom in the chain as a probe atom and examine conditions under which the system may radiate only to those modes whose propagation vectors lie within a small solid angle about the interatomic axis. Such a scheme can be regarded as an atom inside a single-mode cavity.

We find that there is a threshold for the interatomic distances above which a highly directional emission can be achieved. Below the threshold the emission in the horizontal plane is isotropic. However, we find a population trapped in one of the mirror atoms. For the cavitylike arrangement, the directivity function depends strongly on the number of atoms contained in the chain and the distance between them. For a three-atom chain and atomic distances above the threshold, two radiative modes of different spatial directions are available for the emission, one in the direction parallel and the other in the direction normal to the interatomic axis. Below the threshold, the system can radiate only to the mode normal to the interatomic axis. For a five-atom chain and distances above the threshold, only one mode is available for emission, either normal or parallel to the atomic line. Thus, there exist ranges of the interatomic distances under which the atomic chain exhibits features characteristic of a single-mode cavity.

The paper is organized as follows. In Sec. II, we describe the master equation of the density operator of the system and the mathematical approach used in the evaluation of the density matrix elements. We introduce the definitions of the directivity function and reflection and transmission coefficients of the radiation field emitted by a chain of atoms. In Sec. III, we examine the conditions for the mirror-type behavior of short chains composed of three and five atoms. We observe the transient transfer of the population between the atoms and the transient directivity function for an initial condition in which the probe atom is prepared in its excited state. Then we examine the directivity function of the stationary field when the probe atom is driven by a continuous-wave (cw) laser field. Section IV is devoted to the problem of a cavity formation with atomic mirrors. We are particularly interested in the possibility of the system's concentrating the radiation along the interatomic axis and thus behaving as a single-mode cavity. Polar diagrams are given to illustrate the mirror- and cavitylike features of atomic chains and to show how the features are sensitive to the distances between atoms. The results are summarized in Sec. V. The paper concludes with two appendixes. Appendix A gives details of the derivation of the atomic correlation functions in terms of the populations of the collective states of a three-atom system and the coherences among them. The equations of motion for the density matrix elements in a single-photon approximation suitable for numerical evaluation of the radiation intensity are listed in Appendix B.

II. RADIATIVE PROPERTIES OF A CHAIN OF ATOMS

We consider a system composed of N identical two-level atoms located at fixed positions $\vec{r}_i$ and coupled to three-dimensional electromagnetic field whose modes are initially in a vacuum state $|\{0\}\rangle$. Each atom has an excited state $|e_i\rangle$ and a ground state $|g_i\rangle$ separated by energy $\hbar\omega_0$ and connected by a transition dipole moment $\vec{\mu}$.

The atoms are arranged in a line, and we consider two cases shown in Fig. 1. In the first case, illustrated in Fig. 1(a), we assume that the left-side atom, chosen as a "probe" atom is separated from its next neighbor by a distance r_0 which is larger than the separation r_m between the remaining $N-1$ atoms, $r_0 > r_m$. If the probe atom is excited into its upper level, it will spontaneously decay into the ground state, emitting a radiation field that can be absorbed by the chain of closely located atoms and then re-emitted by the atoms towards the probe atom. Thus, the chain of closely located atoms can act as a mirror, directing the emitted radiation into a cone about the interatomic axis and turned towards the probe atom. In the second case, illustrated in Fig. 1(b), we assume that the middle atom in the chain is separated from its adjacent neighbors by a distance r_0 which is much larger than the separation r_m between the remaining atoms. This arrangement may model the situation of an atom located inside a cavity whose mirrors are formed by two chains of equally distant atoms.

In practice this scheme could be realized by extending the recently demonstrated scheme involving two superconducting qubits coupled to a one-dimensional field [31–33] to the case of three or five qubits coupled to a two-dimensional field. In the experiment in Ref. [33], effective separations of λ and $3\lambda/4$

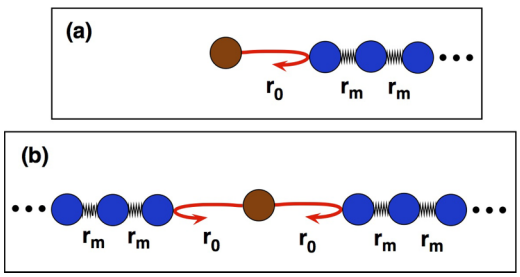

FIG. 1. Two geometrical arrangements of atoms in a line to demonstrate that a chain of closely located and interacting atoms can act as an atomic mirror or cavity. (a) The left-side atom in the chain, specially chosen as a "probe" atom, is located at distance r_0 from its nearest neighbor, with the remaining atoms equally separated from each other by a distance $r_m < r_0$. (b) The middle atom in the chain, chosen as a probe atom, is separated from its next-nearest neighbors by r_0, while the remaining atoms are equally separated by a distance $r_m < r_0$.

were achieved between the fixed qubits by changing the qubit transition frequencies.

A. Master equation

When the system is coupled to a reservoir the state of the total system, the chain of atoms plus the reservoir field, is described by the density operator ρ_T. The reduced density operator describing the properties of only the chain of atoms is obtained by tracing the total density operator ρ_T over the states of the reservoir, $\rho = \mathrm{Tr}_R \rho_T$. The master equation describing the time evolution of the reduced density operator has the form [34–36]

$$\begin{aligned}\frac{\partial \rho}{\partial t} = &-\frac{i}{\hbar}[H_0 + H_L + H_{dd}, \rho] \\ &- \frac{1}{2}\sum_{i=1}^{N} \gamma([S_i^+, S_i^- \rho] + \text{H.c.}) \\ &- \frac{1}{2}\sum_{i\neq j=1}^{N} \gamma_{ij}([S_i^+, S_j^- \rho] + \text{H.c.}),\end{aligned} \tag{1}$$

where γ is the spontaneous emission damping rate of the individual atoms, equal to the Einstein A coefficient, $S_i^+ = |e_i\rangle\langle g_i|$ and $S_i^- = |g_i\rangle\langle e_i|$ are the dipole raising and lowering operators of atom i, and γ_{ij} is the collective damping rate,

$$\begin{aligned}\gamma_{ij} = \frac{3}{2}\gamma\Bigg\{&[1 - (\hat{\mu}\cdot\hat{r}_{ij})^2]\frac{\sin\eta_{ij}}{\eta_{ij}} \\ &+ [1 - 3(\hat{\mu}\cdot\hat{r}_{ij})^2]\left(\frac{\cos\eta_{ij}}{\eta_{ij}^2} - \frac{\sin\eta_{ij}}{\eta_{ij}^3}\right)\Bigg\},\end{aligned} \tag{2}$$

with

$$\eta_{ij} = k\, r_{ij} = 2\pi r_{ij}/\lambda, \quad \vec{r}_{ij} = r_{ij}\hat{r}_{ij} = \vec{r}_j - \vec{r}_i, \tag{3}$$

in which r_{ij} is the distance between atom i and atom j, $\hat{r}_{ij}$ is the unit vector in the direction $\vec{r}_{ij}$, and λ is the resonant wavelength.

The master equation, (1), describes the atomic dynamics under the Born-Markov and rotating-wave approximations [37]; H_0 is the Hamiltonian describing the free energy of the atoms,

$$H_0 = \hbar\sum_{i=1}^{N} \omega_0 S_i^+ S_i^-, \tag{4}$$

and H_L is the Hamiltonian describing the interaction of the probe atom with an external driving field of frequency ω_L,

$$H_L = \tfrac{1}{2}\hbar\Omega_0\left(S_1^+ e^{-i\omega_L t} + S_1^- e^{i\omega_L t}\right), \tag{5}$$

where Ω_0 is the Rabi frequency of the driving field, and H_{dd} is the Hamiltonian describing the dipole-dipole interaction between the atoms,

$$H_{dd} = \hbar\sum_{i\neq j=1}^{N} \Omega_{ij}(S_i^+ S_j^- + S_j^+ S_i^-), \tag{6}$$

where Ω_{ij} is the dipole-dipole interaction strength between atom i and atom j, defined by

$$\begin{aligned}\Omega_{ij} = \frac{3}{4}\gamma\Bigg\{&[1 - 3(\hat{\mu}\cdot\hat{r}_{ij})^2]\left(\frac{\sin\eta_{ij}}{\eta_{ij}^2} + \frac{\cos\eta_{ij}}{\eta_{ij}^3}\right) \\ &- [1 - (\hat{\mu}\cdot\hat{r}_{ij})^2]\frac{\cos\eta_{ij}}{\eta_{ij}}\Bigg\}.\end{aligned} \tag{7}$$

The parameters γ_{ij} and Ω_{ij} depend on the separation between atoms. For large separations, $\eta_{ij} \gg 1$, and both coupling parameters approach 0. For $\eta_{ij} \ll 1$ the parameter γ_{ij} decreases to γ, while Ω_{ij} becomes large and strongly dependent on r_{ij}. It is well known that Ω_{ij} plays an important role in the collective behavior of multiatom systems and we shall see that it has an important effect on the distribution of the radiation field emitted by a chain of atoms. The calculation of the equations of motion for atomic populations and coherences for a time-dependent state vector is outlined briefly in Appendix B.

B. Directivity function and reflection and transmission coefficients

The intensity of the radiation field $\vec{E}(\vec{R},t)$ emitted at time t in the direction specified by the polar angle θ between the direction of observation $\vec{R}$ and the direction of the atomic axis $\vec{r}_{ij}$ and the azimuthal angle ϕ between $\vec{R}$ and the direction of the atomic transition dipole moment $\vec{\mu}_i$ can be expressed in terms of the correlation functions of the atomic dipole operators as [18]

$$\begin{aligned}I(\theta,\phi,t) &= \frac{R^2 c}{2\pi\omega_0}\langle\vec{E}^{(-)}(\vec{R},t)\cdot\vec{E}^{(+)}(\vec{R},t)\rangle \\ &= u(\phi)\sum_{i,j=1}^{N}\gamma\langle S_i^+(t)S_j^-(t)\rangle e^{ikr_{ij}\cos\theta},\end{aligned} \tag{8}$$

where $u(\phi) = (3/8\pi)\sin^2\phi$ is the radiation pattern of a single atomic dipole. In Eq. (8), we have introduced the factor $(R^2c/2\pi\omega_0)$ so that $I(\theta,\phi,t)d\Omega_R dt$ is now the probability of finding a photon inside the solid angle $d\Omega_R$ around the direction $\vec{R}$ in the time interval dt at time t in the far-field zone ($R \gg r_{ij}$) of the radiation emitted by the atoms.

We may introduce the *directivity* function, determining how effective the line of atoms is in converging the emitted radiation into a small solid angle defined by angles θ and ϕ. The directivity function $D(\theta,\phi,t)$ at time t is defined as the ratio of the radiation intensity $I(\theta,\phi,t)$ emitted in the direction (θ,ϕ) divided by the total radiation intensity $I(t)$,

$$D(\theta,\phi,t) = \frac{u(\phi)}{I(t)}\sum_{i,j=1}^{N}\gamma\langle S_i^+(t)S_j^-(t)\rangle e^{ikr_{ij}\cos\theta}, \tag{9}$$

where the total radiation intensity $I(t)$ at time t is obtained by integrating $I(\theta,\phi,t)$ over the solid angle $d\Omega_R$,

$$I(t) = \int I(\theta,\phi,t)d\Omega_R = \sum_{i,j=1}^{N}\gamma_{ij}\langle S_i^+(t)S_j^-(t)\rangle, \tag{10}$$

in which $\gamma_{ii} = \gamma_{jj} = \gamma$ and γ_{ij} $(i \neq j)$ is given in Eq. (2). The directivity function is a measure of how effective the system is in concentrating the radiation into a given direction. It is equivalent to the probability density of detecting a fluorescence photon traveling in the direction specified by θ and ϕ.

Our main interest is in situations where a chain of atoms works as an atomic mirror. Therefore, an important factor is the ability of a line of atoms to concentrate the emitted radiation in one of the two directions along the interatomic axis, either $\theta = 0$ or $\theta = \pi$. Since the radiation of an atomic dipole is

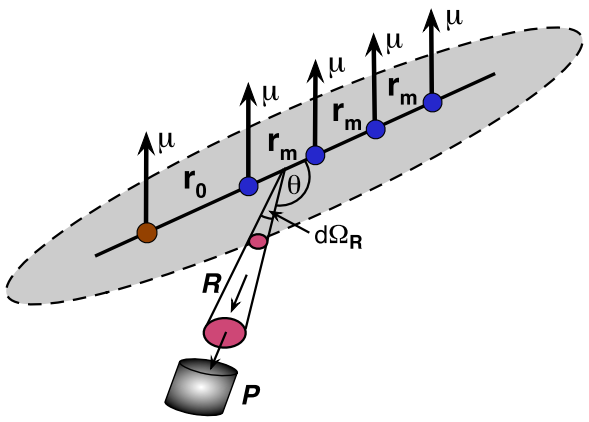

FIG. 2. Geometric arrangement of the atomic dipole moments $\vec{\mu}$ and a photodetector P to monitor the angular distribution of the emitted field. The photodetector detects the emitted field as a function of θ in the plane normal to the direction of the atomic dipole moments ($\vec{R} \perp \vec{\mu}$), the horizontal radiation pattern.

most intense in the direction $\phi = \pi/2$, we consider the angular distribution of the emitted field along a two-dimensional surface normal to the direction of the atomic dipole moments, as illustrated in Fig. 2. In the literature the surface is called the *horizontal radiation pattern*.

Following the arrangement illustrated in Fig. 2, $D(\theta = \pi,\pi/2,t)$ describes the radiation field emitted along the atomic axis in the direction towards the probe atom, the "backward" direction. Thus, it can be interpreted as the field reflected from the atomic mirror. On the other hand, the directivity $D(\theta = 0,\pi/2,t)$ describes the radiation field emitted along the atomic axis in the direction away from the probe atom, the "forward" direction. Therefore, it can be interpreted as the field transmitted through the atomic mirror.

Thus, we may define the *reflection coefficient* of the chain of atoms as the ratio of the radiation scattered in the direction $\theta = \pi$ to the total radiation scattered along the atomic axis,

$$R(t) = \frac{I(\theta = \pi,\pi/2,t)}{I(\theta = 0,\pi/2,t) + I(\theta = \pi,\pi/2,t)}. \tag{11}$$

The reflection coefficient is a measure of how effective the atoms are in concentrating the radiation in the backward direction along the atomic axis, i.e., about the direction $\theta = \pi$. The coefficient $R(t)$ is equivalent to the probability density of detecting a fluorescence photon traveling in the direction $\theta = \pi$.

Similarly, we can define the *transmission coefficient* of the chain as the ratio of the radiation intensity emitted in the direction $\theta = 0$ to the total radiation scattered along the atomic axis,

$$T(t) = \frac{I(\theta = 0,\pi/2,t)}{I(\theta = 0,\pi/2,t) + I(\theta = \pi,\pi/2,t)}. \tag{12}$$

Obviously, $T(t) = 1$ corresponds to the complete forward emission, whereas $R(t) = 1$ indicates the complete backward emission along the atomic axis.

C. Directional properties of the radiation field

We may determine the general conditions under which the horizontal pattern of N atoms would be highly asymmetric, with its maximum concentrated along the atomic axis. Expression (8) can be written as the sum of N terms,

$$I(\theta,\phi,t) = \sum_{i<j=1}^{N} I_{ij}(\theta,\phi,t), \tag{13}$$

where

$$I_{ij}(\theta,\phi,t) = u(\phi)\gamma\left\{\frac{\langle S_i^+(t)S_i^-(t)\rangle + \langle S_j^+(t)S_j^-(t)\rangle}{N-1} + 2\mathrm{Re}\{\langle S_i^+(t)S_j^-(t)\rangle\}\cos(kr_{ij}\cos\theta) - 2\mathrm{Im}\{\langle S_i^+(t)S_j^-(t)\rangle\}\sin(kr_{ij}\cos\theta)\right\}. \tag{14}$$

We see that the contribution of the atoms to the intensity occurs in pairs of different combinations of the atoms. Therefore, the system of radiating atoms can be considered as being made up of a number of short two-atom elements and the total intensity is obtained by summing up the intensities of the fields produced by all the elements.

If we wish a short chain of atoms to work like a mirror with a large convergence and reflectivity of the radiation emitted by a probe atom located at either end of the chain, we should arrange the atoms such that the total field emitted (scattered) can be highly focused along the interatomic axis with a pronounced maximum in the backward direction $\theta = \pi$ and a minimum, preferably zero emission, in the forward direction $\theta = 0$ with respect to the line center. In order to find the conditions for concentrating the radiation in the direction $\theta = \pi$, let us examine the intensity, (14), in more detail.

From Eq. (14) it is seen that there are three terms determining the radiation pattern. The first term in Eq. (14) is just the sum of the populations of the two atoms involved, the probabilities that the atoms are in their excited states. This term is independent of θ and therefore contributes uniformly in all directions. The second term depends on θ and varies as $\cos(kr_{ij}\cos\theta)$, with an amplitude equal to the real part of atomic correlations. Consequently, this term can contribute to the radiation pattern only if the correlations between the atoms have nonzero real part, $\mathrm{Re}\{\langle S_i^+ S_j^-\rangle\} \neq 0$. However, the cosine term $\cos(kr_{ij}\cos\theta)$ attains the maximum value (=1) for directions determined by $kr_{ij}\cos\theta = 0,2\pi$. Therefore, it would produce intensity maxima in the $\theta = \pi/2,3\pi/2$ and $\theta = \arccos(\lambda/r_{ij})$ directions. As such, this term is not effective in concentrating the radiation along the interatomic axis. This simple argument suggests that the atoms should be arranged so that the cosine term vanishes. This can be achieved when the correlations between the atoms have zero real part.

The third term contributing to the radiation intensity, (14), varies as $\sin(kr_{ij}\cos\theta)$ and hence can affect the radiation intensity in a decidedly different way than the cosine term. An important difference is that $\sin(kr_{ij}\cos\theta)$ vanishes for $\theta = \pi/2$ and $3\pi/2$. This means that the sine term does not contribute to the radiation emitted in the direction perpendicular to the interatomic axis. Consequently, an appreciable concentration of the radiation can be achieved along the

interatomic axis by choosing proper distances r_{ij} between the atoms at which $\sin(kr_{ij}) = \pm 1$. Furthermore, since the sine is an odd function, it follows that $\sin(kr_{ij}\cos 0^\circ) = -\sin(kr_{ij}\cos 180^\circ)$, which means that, independent of the separation between the atoms, a maximum in the backward direction is always accompanied by a minimum in the forward direction.

Obviously, the sine term can influence the angular distribution of the radiation intensity only if the atomic correlations have nonzero imaginary parts, $\mathrm{Im}\{\langle S_i^+ S_j^-\rangle\} \neq 0$. In addition, the sign of the imaginary part of the atomic correlations dictates the choice of distances between the atoms at which the emission will be enhanced in the backward direction (high reflection) and reduced in the forward direction (low transmission). Thus, if $\mathrm{Im}\{\langle S_i^+ S_j^-\rangle\} > 0$, the sine term will display a maximum in the backward direction for atomic distances at which $\sin(kr_{ij}) = 1$. This condition is satisfied when the atomic separations are

$$r_{ij} = \tfrac{1}{4}(2n+1)\lambda, \quad n \in \{0,2,4,\ldots\}. \tag{15}$$

However, if the coefficient of the sine term is negative, $\mathrm{Im}\{\langle S_i^+ S_j^-\rangle\} < 0$, a different choice of distances is required at which $\sin(kr_{ij}) = -1$. This condition is satisfied when

$$r_{ij} = \tfrac{3}{4}(2n+1)\lambda, \quad n \in \{0,2,4,\ldots\}. \tag{16}$$

We see that there is a lower bound imposed on the distances between the atoms, either $r_{ij} = \lambda/4$ or $r_{ij} = 3\lambda/4$, above which a one-sided emission along the interatomic axis can be achieved, i.e., a maximum of radiation in the direction $\theta = 0$. For distances shorter than the lower bound, the one-sided emission is expected to be significantly reduced.

In the following, we limit ourselves to short chains containing only $N = 3$ and $N = 5$ atoms. Also in the absence of the driving field, $\Omega_0 = 0$, the $N = 3$ case can be solved in closed form yielding simple mathematical expressions. In Appendix A, we outline the calculation of the atomic correlation functions in the collective state basis.

D. Mathematical approach

To study the radiative behavior of a chain of interacting atoms, we require the time evolution of the populations of atoms and the coherences between them. These are given by the diagonal and off-diagonal density matrix elements, respectively. If the space of the atomic system is spanned in the basis of the eigenstates of the free Hamiltonian H_0, we readily find that the basis is composed of 2^N state vectors, i.e., for a chain composed of $N = 3$ atoms, the basis is composed of 8 vectors $|i_1 j_2 k_3\rangle$, whereas for $N = 5$ atoms it is composed of 64 vectors $|i_1 j_2 k_3 l_4 m_5\rangle$, $\{i,j,k,l,m\} \in \{g,e\}$.

Hence, in the simplest case of $N = 3$ atoms, the master equation, (1), provides us with a system of 64 coupled linear equations to be solved, in principle, a 63×63 matrix to be diagonalized. For $N = 5$ there are a total of 4096 coupled linear equations whose solution requires the diagonalization of a 4095×4095 matrix.

If initially the probe atom is prepared in a single excitation state or is driven by a weak laser field, the space of the atomic system can be truncated to the ground and single excitation states only. The truncated basis of $N = 3$ and $N = 5$ atoms is spanned by four and six state vectors, respectively. This significantly reduces the computation time. For example, the case of $N = 3$ requires 16×16, whereas the case of $N = 5$ requires a 64×64 matrix to be diagonalized.

To get solutions for the density matrix elements, in both the truncated and the complete basis, the following approach is taken. From the master equation, (1), we find equations of motion for the density matrix elements, which can be written in matrix form as

$$\dot{\vec{X}}(t) = \mathcal{A}\vec{X}(t) + \vec{R}, \tag{17}$$

where $\vec{X}(t)$ is a column vector composed of the density matrix elements, $\vec{R}$ is a column vector composed of the inhomogeneous terms, and $\mathcal{A}$ is a matrix of the coefficients appearing in the equations of motion of the density matrix elements.

Direct integration of Eq. (17) leads to the formal solution for $\vec{X}(t)$,

$$\vec{X}(t) = \vec{X}(t_0)e^{\mathcal{A}t} - (1 - e^{\mathcal{A}t})\mathcal{A}^{-1}\vec{R}, \tag{18}$$

where t_0 is the initial time. Because the determinant of matrix $\mathcal{A}$ is different from 0, there exists a complex invertible matrix $\mathcal{U}$ which diagonalizes $\mathcal{A}$, and $w = \mathcal{U}^{-1}\mathcal{A}\mathcal{U}$ is the diagonal matrix of complex eigenvalues. By introducing new vectors, $\vec{Y} = \mathcal{U}^{-1}\vec{X}$ and $\vec{T} = \mathcal{U}^{-1}\vec{R}$, we can rewrite (18) as

$$\vec{Y}(t) = \vec{Y}(t_0)e^{wt} - (1 - e^{wt})w^{-1}\vec{T} \tag{19}$$

or, in component form,

$$Y_n(t) = Y_n(t_0)e^{w_n t} - \sum_{m=1}^{s}(w^{-1})_{nm}(1 - e^{w_m t})T_m, \tag{20}$$

in which $s = 63$ for the case of $N = 3$ atoms and $s = 4095$ for $N = 5$ atoms in the complete basis. To obtain solutions for $X_n(t)$ we must determine the eigenvalues w_n and eigenvectors $Y_n(t)$, which are readily evaluated by a numerical diagonalization of matrix $\mathcal{A}$.

The steady-state values of the density matrix elements can be found from Eq. (20) by taking $t \to \infty$ or, more directly, by setting the left-hand side of Eq. (17) equal to 0, and then

$$\vec{X}(\infty) = -\mathcal{A}^{-1}\vec{R} \tag{21}$$

or, in component form,

$$X_n(\infty) = -\sum_{m=1}^{s}(\mathcal{A}^{-1})_{nm}R_m. \tag{22}$$

In what follows, we use solutions (20) and (22) to illustrate the radiative properties of the atomic chains. In particular, we calculate the transient populations of the atoms and the steady-state directivity function.

III. RADIATING ATOM IN FRONT OF AN ATOMIC MIRROR

Consider first the configuration illustrated in Fig. 1(a): a single atom is positioned at a distance r_0 from a finite-size chain of closely located atoms. This arrangement can constitute a radiating atom in front of an atomic mirror. In order to find the mirrorlike characteristics of the chain that

can be inferred from the radiative properties of the system, we examine the directivity function of the radiation field emitted by the system. The directivity function, which is determined by the angular distribution of the radiation intensity, Eq. (13), depends on temporal and spatial factors, the evolution time of the system and the separation between atoms. It is clear from Eq. (13) that in general the temporal and spatial factors cannot be separated. The angular distribution of the radiation field at a given time can be different for different separations between atoms. Moreover, the transient radiation intensity is a sensitive function of the initial atomic conditions. Even at the initial time $t = 0$ the angular distribution of the radiation intensity can depend on the separation r_{ij} if the system was prepared in a state with nonzero interatomic correlations, i.e., either $\mathrm{Re}\{\langle S_i^+ S_j^-\rangle\}$ or $\mathrm{Im}\{\langle S_i^+ S_j^-\rangle\}$ different from 0. In order to study the angular distribution of the radiation field, it is important to understand the radiative behavior of individual atoms in the chain. Therefore, we first consider the time evolution of the populations of atoms. Following this discussion, we display the variation of the directivity function with time for different distances between atoms. We assume that the probe atom is initially excited and separated from the front atom of the "mirror," its nearest neighbor, at a distance much longer than the separation between the mirror atoms. The method of preparing the probe atom in the excited state does not concern us, but it might be done with a short laser pulse, for example.

A. Transient transfer of the population

Our interest is in the time evolution of the directivity function of the emitted field for an initially excited probe atom, the case illustrated in Fig. 1(a). In order to study this evolution, we first look at the time evolution of the populations of atoms for chains composed of $N = 3$ and $N = 5$ atoms. The aim is to first determine and then optimize the conditions which allow the radiation emitted by the probe atom not only to be emitted back (reflected) to it but also to achieve a strong convergence of the radiated field along the interatomic axis.

We evaluate the transient populations of the atoms assuming there is no driving field ($\Omega_0 = 0$) and that initially the probe atom was in its excited state. The corresponding results for the time evolution of the atomic populations for different distances between atoms are presented in Figs. 3 and 4.

Figure 3 shows the transient transfer of the population between $N = 3$ atoms: the initially excited probe atom and a group of two atoms forming a mirror. The populations are computed for several sets of distances (r_0, r_m) between atoms. For distances $r_0, r_m > \lambda/5$ the initial population of the probe atom decays exponentially in time, whereas the populations of mirror atoms 2 and 3 increase with small oscillations. However, there is no tendency of the mirror atoms to transfer their populations back to the probe atom. A small oscillatory behavior of the population $\rho_{11}(t)$ can be seen for short times, $t < 5/\gamma$, but it is not periodic.

Periodic oscillatory behavior is observed for the populations of atoms 2 and 3. The mirror atoms periodically exchange their populations without transferring them to the probe atom. The reason is that the distance r_m is much smaller than r_0, resulting in a stronger dipole-dipole interaction between the mirror atoms, $\Omega_{23} \gg \Omega_{12}$. For shorter distances,

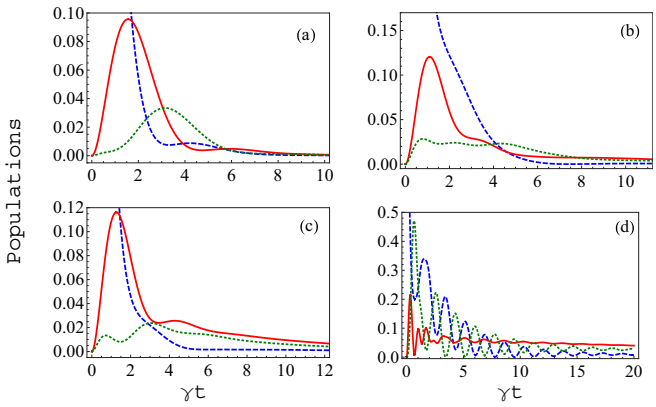

FIG. 3. Time evolution of the atomic populations $\rho_{11}(t)$ (dashed blue line), $\rho_{22}(t)$ (solid red line), and $\rho_{33}(t)$ (dotted green line) plotted for the case of an initially excited probe atom, 1, located in front of a line of two atoms, 2 and 3, and several sets of distances between atoms: (a) $(r_0, r_m) \in (\lambda/2, \lambda/4)$, (b) $(r_0, r_m) \in (\lambda/4, \lambda/6)$, (c) $(r_0, r_m) \in (\lambda/3, \lambda/5)$, and (d) $(r_0, r_m) \in (\lambda/8, \lambda/9)$.

the population of the probe atom begins to show periodic oscillations, with the population actually oscillating between the probe atom and only the rear atom of the mirror. Except at very short times, the population of the middle atom, 2, remains almost constant during the evolution of the system. Note that the transfer of the population between atoms is not complete since the populations remain nonzero, $\rho_{ii}(t) \neq 0$, for all $t > 0$. It is interesting that atom 2, the front atom of the mirror, appears as a mediator in the population exchange between the probe atom and the rear atom of the mirror. In other words, the front atom of the mirror dictates the direction of the emission. Despite its ability to emit in any spatial direction, the probe atom "prefers" to radiate towards the atomic mirror, and vice versa, the mirror atoms prefer to radiate towards the probe atom.

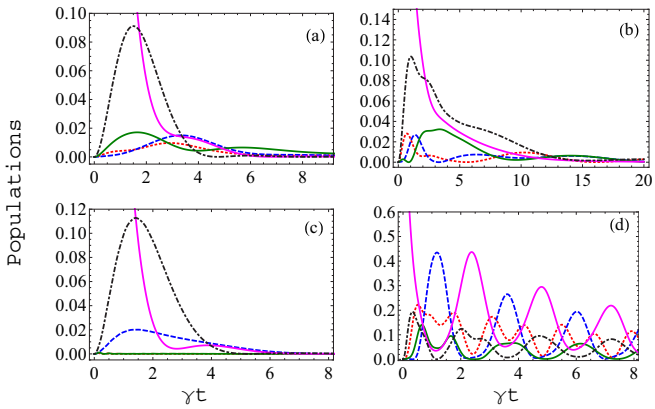

FIG. 4. Time evolution of the atomic populations, ρ_{11} (solid magenta line), ρ_{22} (dashed-dotted black line), ρ_{33} (dotted red line), ρ_{44} (solid green line), and ρ_{55} (dashed blue line) plotted for the case of an initially excited probe atom, 1, located in front of a line of four atoms and several sets of distances between atoms: (a) $(r_0, r_m) \in (\lambda/2, \lambda/4)$, (b) $(r_0, r_m) \in (\lambda/4, \lambda/6)$, (c) $(r_0, r_m) \in (\lambda/3, \lambda/5)$, and (d) $(r_0, r_m) \in (\lambda/8, \lambda/9)$.

We now consider a chain containing $N = 5$ atoms, with the probe atom initially excited and located at a distance r_0 from the front of a line of four equally separated atoms. The transient transfer of the population between atoms for several sets of distances, (r_0,r_m), is shown in Fig. 4. For large distances the situation is similar to that of three atoms; the population rapidly escapes from the system, leaving the atoms unpopulated over a short evolution time. For small distances, we observe periodic oscillations of the populations with the periodicity, as before for three atoms, determined by the dipole-dipole interaction strength. However, unlike the three-atom case, the population can be completely transferred from the mirror atoms back to the probe atom such that the mirror atoms are unpopulated at times when the population of the probe atom is maximal. This is a substantial difference compared to the case of $N = 3$ atoms, where a part of the population was trapped by one of the mirror atoms. Clearly, longer chains are more effective in the complete transfer of an excitation from the probe atom to the mirror atoms, and vice versa.

The results presented in Figs. 3 and 4 show that the fast periodic exchange of excitation between atoms is not confined to times short compared with the relaxation time γ^{-1}, and its magnitude increases with the strength of the dipole-dipole interaction. For a strong coupling between atoms, the initial population disappears in a time longer than the decay time of the atoms.

B. Transient directivity function

The periodic exchange of the populations between atoms, in particular, between atoms forming an atomic mirror, can lead to the emission of atoms into certain preferred directions. In order to demonstrate this behavior, we examine the time variation of the directivity function $D(\theta,\pi/2,t)$ of the field radiated by the group of mirror atoms only. Of course it might be argued that it would be hard for experiments to detect the field radiated from a fraction of atoms, but we would like to see under what conditions the field radiated by the group of mirror atoms could be concentrated in the preferred direction along the interatomic axis, either $\theta = 0$ or $\theta = \pi$. With a high concentration of the radiated field in a small solid angle centered around $\theta = 0$, the atoms can be regarded as a highly reflecting mirror scattering the field back towards the probe atom.

The directionality function of the field emitted by two (mirror) atoms and detected on a sphere around the line of three atoms is shown in Fig. 5. We keep the distance of the probe atom from the front of the mirror atoms at $r_0 = \lambda/2$ and consider the variation of $D(\theta,\pi/2,t)$ with the distance between the mirror atoms at two times. It is seen that the emission is concentrated along the interatomic axis. For a distance between the mirror atoms $r_m = \lambda/4$, the directivity function is significantly enhanced in one direction, and the emission is almost one-sided in either $\theta = 0$ or $\theta = \pi$. The maximum of the directivity function oscillates in time along the inter atomic axis. The oscillation of the directivity results from the oscillation of the population between mirror atoms, as shown in Fig. 3. The beam width or, equivalently, the solid angle inside which the emitted field is concentrated remains almost constant.

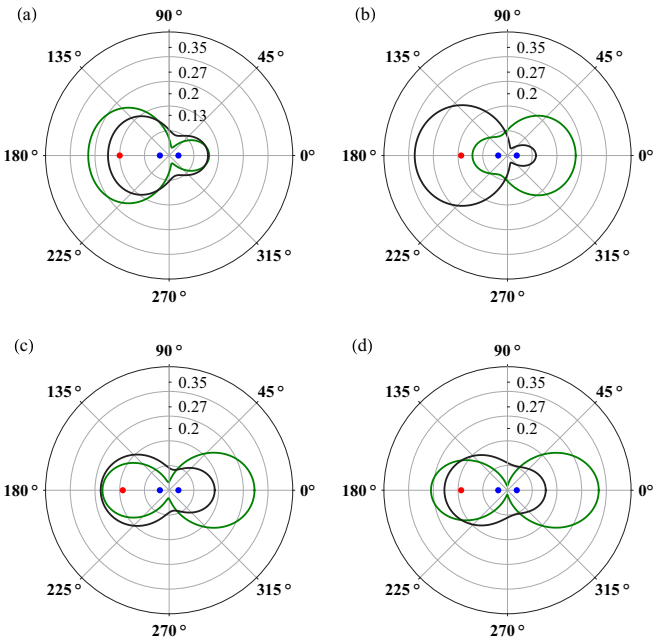

FIG. 5. Polar diagram of the directivity function $D(\theta,\pi/2,t)$ describing the concentration of the field emitted by two atoms forming a mirror when an initially excited probe atom is at distance $r_0 = \lambda/2$ from the front of the mirror atoms. Distances between mirror atoms are (a) $r_m = \lambda/3$, (b) $r_m = \lambda/4$, (c) $r_m = \lambda/5$, and (d) $r_m = \lambda/8$. The green (black) curve corresponds to a minimum (maximum) in $\rho_{11}(t)$. The instants in time for the green and black curves are (a) $t \in \{3\gamma^{-1},4\gamma^{-1}\}$, (b) $t \in \{5\gamma^{-1},3.3\gamma^{-1}\}$, (c) $t \in \{9\gamma^{-1},3.6\gamma^{-1}\}$, and (d) $t \in \{9.4\gamma^{-1},6\gamma^{-1}\}$, respectively.

One can also notice in Fig. 5 that the ability of the coupled atoms to concentrate the radiation in one direction decreases with decreasing distance between the atoms. It is clearly shown that for distances $r_m \leqslant \lambda/8$ the directivity function is almost symmetrical along the interatomic axis. This result is consistent with the general property of the radiation pattern discussed in Sec. II B that there is a minimal value of the distance between atoms ($r_m = \lambda/4$) above which the sine term can be maximal in the $\theta = 0$ direction. For distances smaller than the minimal value the contribution of the sine term is necessarily smaller, resulting in a reduction in the ability of the system to concentrate the emission in one direction.

The one-sided emission and then the reflectivity coefficient can be enhanced by increasing the number of atoms forming the atomic mirror. This is demonstrated in Fig. 6, which shows a polar diagram of the directivity function $D(\theta,\pi/2,t)$ for the case of four atoms forming the atomic mirror. As above for three atoms, we keep the probe atom at a fixed distance from the front of the atomic mirror, $r_0 = \lambda/2$, and consider the variation of $D(\theta,\pi/2,t)$ with the distance between mirror atoms. It can be seen that, similarly to the case of two atoms, the emission is concentrated mainly along the interatomic axis. The one-sided emission is significantly enhanced and persists even for short distances. Small peaks can be seen at about $2\pi/3\,^\circ$ and $4\pi/3\,^\circ$. It is easy to verify that the function $\sin(kr_{ij}\cos\theta)$, when evaluated for $r_{ij} = 3r_m = 3\lambda/8$, corresponding to the distance between the front and the rear atoms of

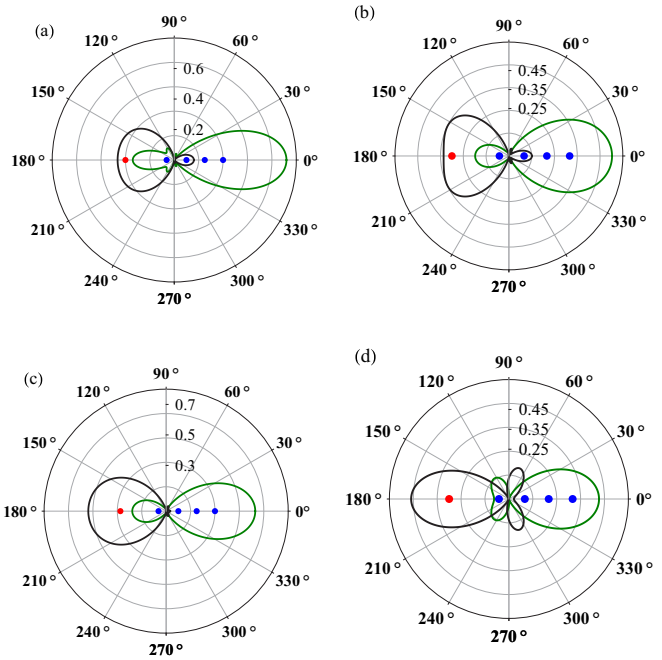

FIG. 6. Polar diagram of the directivity function $D(\theta,\pi/2,t)$ describing the concentration of the field emitted by four atoms forming a mirror when an initially excited probe atom is at distance $r_0 = \lambda/2$ from the front of the mirror atoms. Distances between mirror atoms are (a) $r_m = \lambda/3$, (b) $r_m = \lambda/4$, (c) $r_m = \lambda/5$, and (d) $r_m = \lambda/8$. The green (black) curve corresponds to a minimum (maximum) in $\rho_{11}(t)$. The instants in time for the green and black curves are (a) $t \in \{7.76\gamma^{-1},3.7\gamma^{-1}\}$, (b) $t \in \{6.8\gamma^{-1},3.4\gamma^{-1}\}$, (c) $t \in \{7\gamma^{-1},3.715\gamma^{-1}\}$, and (d) $t \in \{7.6\gamma^{-1},9.1\gamma^{-1}\}$, respectively.

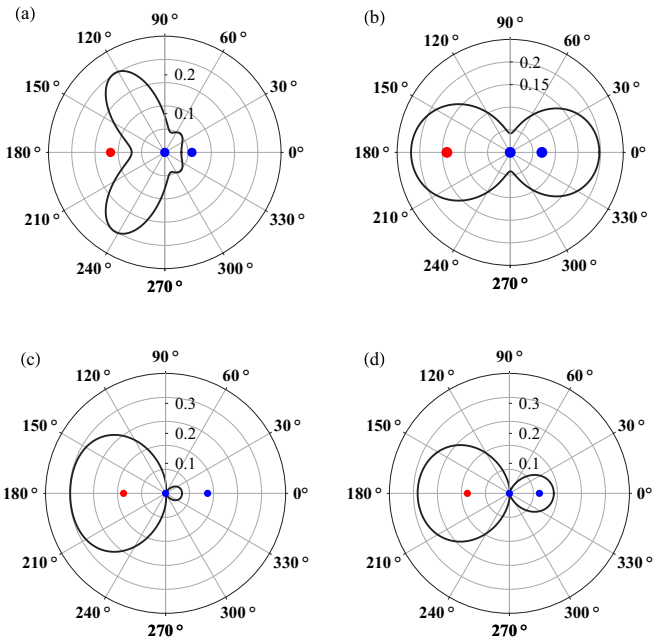

FIG. 7. Polar diagram of the directivity function $D(\theta,\pi/2)$ of the stationary field emitted by three atoms in a line. The leftmost atom in the line, which constitutes a probe atom, is driven by a cw laser field of Rabi frequency $\Omega_0 = 0.02\gamma$. (a) $r_0 = \lambda/2, r_m = \lambda/4$; (b) $r_0 = \lambda/4, r_m = \lambda/8$; $r_0 = r_m = \lambda/4$; and (d) $r_0 = \lambda/4, r_m = \lambda/6$.

the mirror, attains its maximal value of $\sin(kr_{ij}\cos\theta) = 1$ for $\cos\theta = 2/3$, which corresponds to directions $\theta \approx 130^\circ$.

C. Directivity function of the stationary field

In practice a photodetector located at some position $\vec{R}$ in the far-field zone of the radiation field emitted by the atoms would detect the field emitted by the entire set of atoms rather than a fraction of selected atoms only. This is a consequence of the fact that the fields from the probe atom and the mirror atoms are unresolved at the detector. Therefore, we now consider the directivity function of the field radiated by the entire system of atoms including the field radiated from the probe atom. Moreover, we assume that initially all atoms were in their ground states and then the probe atom was exposed to the incident weak laser light. We look into the radiation pattern of the emitted field in the steady-state limit, $t \to \infty$, and compute the directivity function $D(\theta,\pi/2) \equiv \lim_{t\to\infty} D(\theta,\pi/2,t)$ for equally distant as well as for not equally distant $N = 3$ and $N = 5$ atoms. Since the directivity function involves the contribution from the populations of atoms, significant directionality can be obtained when the populations are small, and we assume that the driving field is weak so that the Rabi frequency Ω_0 is much smaller than γ. We use the complete and truncated basis states in the calculations and find that both cases lead to the same results.

The directivity function for the radiation field emitted by $N = 3$ atoms is shown in Fig. 7, where Fig. 7(a) is for distance $r_0 = \lambda/2$, while Figs. 7(b)–7(d) are for distance $r_0 = \lambda/4$. It is shown that $D(\theta,\pi/2)$ depends crucially on the separation between atoms. In particular, when the probe atom is separated from the front of the mirror atoms by $r_0 = \lambda/2$ the stationary field radiated by the system is concentrated in directions $\theta = \pi/3$ and $\theta = 5\pi/3$, which depart significantly from the direction of the interatomic axis. However, for $r_0 = \lambda/4$ the emission is concentrated along the interatomic axis.

Figure 8 shows the corresponding situation for the case of $N = 5$ atoms. It is shown that in the case of $r_0 = \lambda/4$, the radiated field modes available for emission are only those contained inside a cone centered about the direction $\theta = \pi$. Thus, at that particular distance the chain of four undriven atoms acts as a perfectly reflecting mirror by "pushing" the radiation in the backward direction. It can be seen that the optimal conditions for one-sided emission with a maximum in the direction $\theta = \pi$ are achieved when the probe atom is separated from the front of the mirror atoms by $r_0 = \lambda/4$ and the mirror atoms are themselves separated by $r_m = \lambda/6$. In this case, the directivity function is nonzero only in directions contained inside a cone limited by $\theta \leqslant \pm\pi/3$. Thus, the emission is entirely one-sided, with no radiation in the $\theta = 0$ direction. This means that the transmission coefficient $T = 0$, therefore this type of behavior can be regarded as a mirror type with perfect reflectivity. Of course, the reflectivity is accompanied by losses in the sense that the radiation is emitted into a cone of a finite solid angle 2θ determining the beam width of the radiated field. The solid angle subtended by the cone shown in Fig. 8(c) is $2\theta = 120^\circ$.

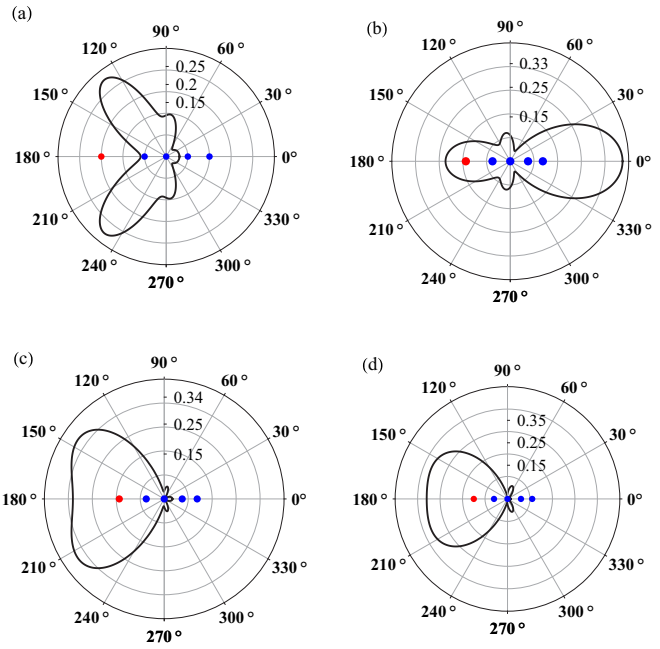

FIG. 8. Polar diagram of the directivity function $D(\theta,\pi/2)$ of the stationary field radiated by a line of five atoms. The leftmost atom in the line, which constitutes a probe atom, is driven by a cw laser field of Rabi frequency $\Omega_0 = 0.02\gamma$. (a) Atoms are unequally separated with $r_0 = \lambda/2$, and $r_m = \lambda/4$. (b) Atoms are unequally separated with $r_0 = \lambda/4$, and $r_m = \lambda/8$. (c) Atoms are equally separated with $r_0 = r_m = \lambda/4$. (d) Atoms are unequally separated with $r_0 = \lambda/4$, and $r_m = \lambda/6$.

It was pointed out in [26] that a strong directivity of the emitted radiation along the interatomic axis can be obtained in a chain of independent atoms, i.e., in the absence of the dipole-dipole interaction. However, the one-sided emission shown in Figs. 8(c) and 8(d) requires a nonzero dipole-dipole interaction. This is illustrated in Fig. 9, which shows the directivity function for the same parameters as in Fig. 8(d) but for independent atoms. Clearly, in the absence of the dipole-dipole interaction between atoms, the emission is strongly directional but is symmetrical in the $\theta = 0$ and π directions.

Finally, we briefly comment on the role of quantum fluctuations in the directivity of the emitted field. If we examine the steady-state values of the averages appearing in Eq. (14), we find that under the weak driving considered here ($\Omega_0 = 0.02\gamma$), the correlation functions factorize, i.e., $\langle S_i^+(t)S_j^-(t)\rangle = \langle S_i^+(t)\rangle\langle S_j^-(t)\rangle$. We see that under weak excitation the scattered light is coherent in the steady state such that quantum fluctuations are 0 [38]. In physical terms, the atomic dipoles behave similarly to classical dipoles.

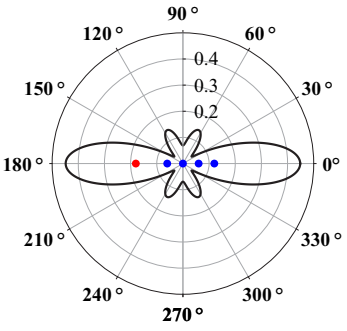

FIG. 9. Polar diagram of the directivity function $D(\theta,\pi/2)$ of the stationary field radiated by a line of five independent atoms ($\Omega_{ij} = 0$). Atoms are unequally separated with $r_0 = \lambda/4$, and $r_m = \lambda/6$.

In summary of this section, we have seen that the directivity of the emission and the mirrorlike behavior of a line of atoms depends on the distance between atoms and the nature of the excitation. At particular distances between atoms, the system can radiate along the interatomic axis in only one direction, $\theta = \pi$, which can be interpreted as a perfect reflection of the radiation towards the probe atom.

IV. CAVITY FORMATION WITH ATOMIC MIRRORS

We now wish to create a cavity with atomic mirrors. For this purpose, we place a probe atom between a pair of finite-size chains of closely located atoms, as illustrated in Fig. 1(b). These will constitute a radiating atom located inside a one-dimensional cavity. We determine the parameter ranges in which the two chains of $(N-1)/2$ atoms can act as mirrors to the field emitted by the probe atom. We examine two systems containing different numbers of atoms. First, we consider the simplest system, composed of $N = 3$ equidistant atoms in a line. Then we extend our discussion to a larger system, composed of $N = 5$ atoms. We illustrate our considerations by examining the time evolution of the atomic populations. For the initial conditions we choose the middle (probe) atom to be in its excited state and the other atoms to be in their ground states. We also analyze the directivity function for features indicative of cavity-type modifications of the radiation pattern of the radiation field.

A. Transient regime

The simplest system which can exhibit features characterizing a cavity formed by atomic mirrors is a chain of $N = 3$ equidistant atoms. Let us first examine the process of population transfer between the middle (probe) atom of the chain and the side (mirror) atoms. The time evolution of the populations of the atoms is illustrated in Fig. 10, where we present the dependence of the population transfer on the distance between atoms. It is shown that the population is periodically transferred between the probe atom and the mirror atoms. The transfer occurs at a frequency determined by the dipole-dipole coupling Ω_{12} ($= \Omega_{23}$) between the probe and the mirror atoms. The oscillations show the interesting behavior that the population transfer is not affected (modulated) by the presence of the dipole-dipole coupling Ω_{13} between the mirror atoms.

The oscillations are accompanied by a steady decay of the populations. However, depending on the distance between atoms, the populations may not decay to 0 but, rather, to long-lived nonzero values. It is clearly shown in Fig. 10 that for atomic distances $r_0 < \lambda/4$, i.e., the spacing between the mirror atoms $2r_0 < \lambda/2$, a significant part of the initial population remains trapped in the probe atom, from which it decays very slowly. We thus have a situation similar to that encountered in a

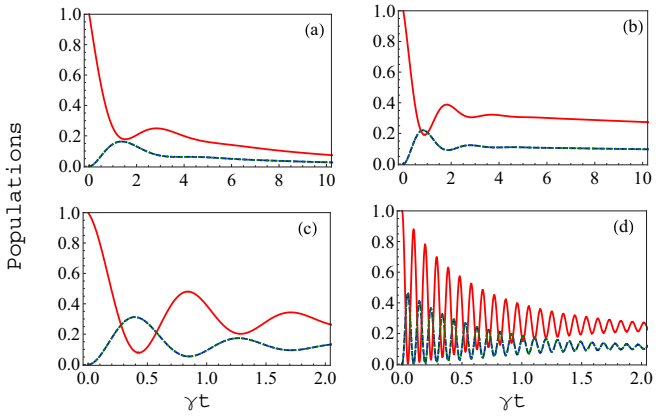

FIG. 10. Time evolution of the atomic populations, ρ_{22} (solid red line), ρ_{11} (dashed blue line), and ρ_{33} (dotted green line), plotted for the cavity-type configuration of three atoms and for different distances between atoms: (a) $r_0 = \lambda/4$, (b) $r_0 = \lambda/6$, (c) $r_0 = \lambda/8$, and (d) $r_0 = \lambda/16$. Initially, the middle (probe) atom, 2, was excited, $|\psi(0)\rangle = |2\rangle$.

Fabry-Pérot cavity composed of a pair of parallel-plate mirrors [39]. In the cavity, the number of modes for interaction with an atom decreases with decreasing separation L between the mirrors. For $L < \lambda/2$ the number of modes is suppressed, resulting in the suppression of the radiation from the atom.

Figure 11 illustrates the cavitylike situation involving five atoms. Here, each of the cavity mirrors is formed with two atoms. The results are similar to those we encountered for the case of three atoms (Fig. 10), however, one can see some interesting differences. Again, trapping of the population for short distances between atoms is evident. It is noteworthy that the system has a tendency to trap the population in the mirror atoms rather than in the probe atom. It can also be noted that for long distances the probe atom exchanges the population with its next neighbors, the front atoms, rather than with the rear atoms forming the mirrors. However, for short distances,

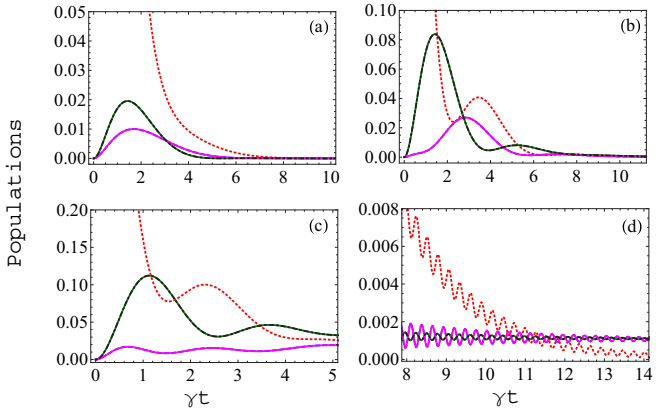

FIG. 11. Time evolution of the atomic populations plotted for the cavity-type configuration of a chain of five atoms and different distances between atoms: (a) $r_m = \lambda/2$, $r_0 = \lambda$; (b) $r_m = \lambda/4$, $r_0 = \lambda/2$; (c) $r_m = \lambda/6$, $r_0 = \lambda/3$; and (d) $r_m = \lambda/16$, $r_0 = \lambda/8$. Initially, the middle (probe) atom, 3, was excited, $|\psi(0)\rangle = |3\rangle$. Color and style specifications as in Fig. 4.

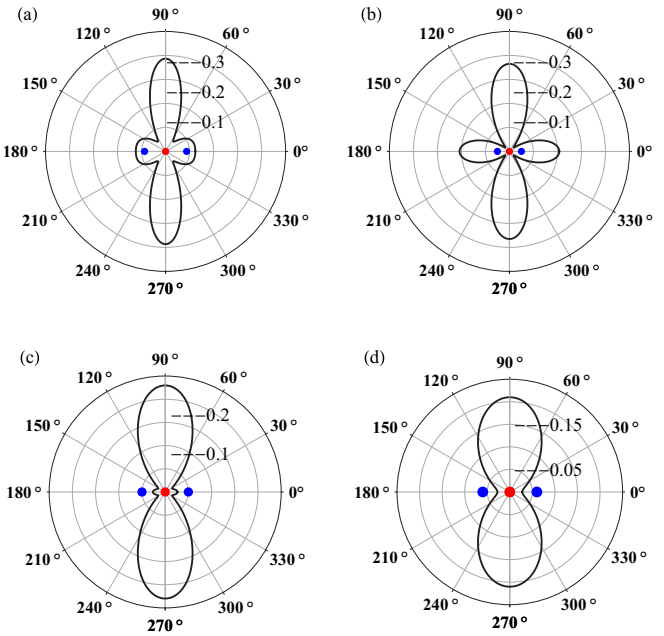

FIG. 12. Polar diagram of the directivity function $D(\theta,\pi/2)$ of the stationary field in the cavitylike situation involving three atoms. The middle atom, which constitutes a probe atom, is driven by a cw laser field of Rabi frequency $\Omega_0 = 0.02\gamma$. The atoms are separated by (a) $r_0 = \lambda/2$, (b) $r_0 = \lambda/4$, (c) $r_0 = \lambda/5$, and (d) $r_0 = \lambda/6$.

the probe atom exchanges the population with the rear atoms, leaving the populations of the front atoms almost constant in time. Similar effects appeared in the population transfer in the system composed of a probe atom located at the front of an atomic mirror (see Sec. III A).

B. Stationary regime

We now turn to the problem of determining the conditions under which the two chains of atoms can act like cavity mirrors to select modes centered about the atomic axis as the only modes available for emission. We assume that the probe atom is continuously driven by a coherent laser field and consider the field in the steady-state limit.

Figure 12 illustrates the effect of decreasing distance between atoms on the directivity function $D(\theta,\pi/2)$ of the stationary field for the cavitylike situation involving three atoms. It is shown that the directivity function is very sensitive to the distances between atoms. For large distances, the system radiates along the cavity axis as well as in the direction normal to the cavity axis. When the atomic separations are reduced below $\lambda/4$, which corresponds to a mirror-atom spacing of less than $\lambda/2$, we see a cancellation of the radiation along the interatomic axis. Thus, the system turns off the radiation along the cavity axis. It radiates only in the directions normal to the cavity axis, a property which clearly is not characteristic of a cavity.

Turning next to the case of five atoms, we plot in Fig. 13 the directivity function for several distances between atoms. We see that the directivity function differs significantly from what we observed for the case of three atoms. Thus, the effect of additional atoms in forming the cavity mirrors is clearly more

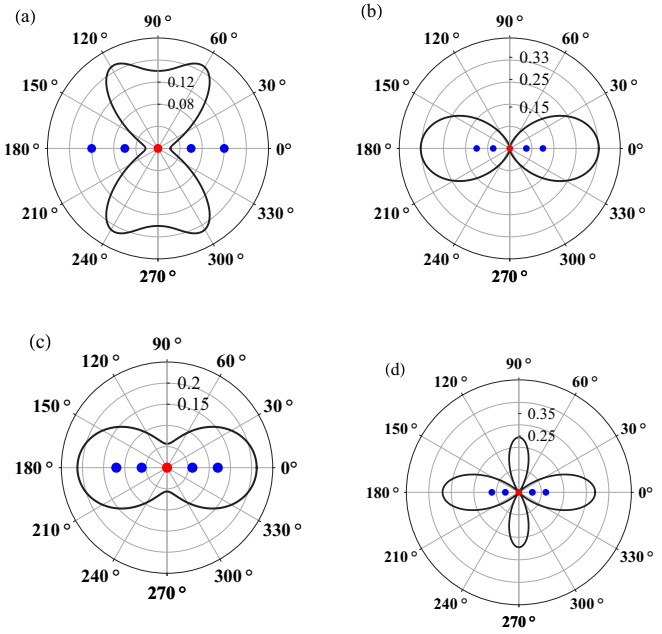

FIG. 13. Polar diagram of the directivity function $D(\theta,\pi/2)$ of the stationary field in the cavitylike situation involving five atoms. The middle atom, which constitutes a probe atom, is driven by a cw laser field of Rabi frequency $\Omega_0 = 0.02\gamma$. (a) The probe atom is separated from its next-nearest neighbors by $r_0 = \lambda/2$, while the atoms which constitute the cavity mirrors are separated by $r_m = \lambda/4$; (b) $r_0 = \lambda/4$ and $r_m = \lambda/8$; (c) $r_0 = \lambda/4$ and $r_m = \lambda/10$; (d) $r_0 = \lambda/8$ and $r_m = \lambda/8$.

pronounced on the directivity function of the stationary field than on the transient population of the atoms. First, we note from the figure that there are distances between atoms at which the directivity function is nonzero only along the interatomic axis [Figs. 13(b) and 13(c)].

It can also be noted that there is an optimal distance between the mirror atoms at which the solid angle subtended by the cone is minimal or, equivalently, the width of the cavity axial mode is very narrow. As shown in Fig. 13(c), a reduction in the separation may result in an increase in the beam width. We also see quite clearly that with larger separations between mirror atoms, additional directions of emission appear [Fig. 13(d)].

V. SUMMARY

We have studied the directional properties of the radiation field emitted by a chain of closely located and dipole-dipole-interacting two-level atoms. Two geometrical configurations of atoms in the chain have been studied: a probe atom in front of a finite-size chain of closely located atoms and a probe atom between a pair of chains of closely located atoms. We call the former case an atom in front of an atomic mirror and the latter an atom inside a cavity where the mirrors are formed by two chains of atoms. We have found that it is possible to account for certain mirror- and cavitylike features. We have examined the conditions for one-sided emission centered about the interatomic axis and have found a lower bound for the distances between atoms above which a one-sided emission along the interatomic axis can be achieved. The one-sided emission focused into a cone about the interatomic axis and oriented in the backward direction can be regarded as a mirror type with perfect reflectivity. For interatomic distances smaller than the lower bound, a part of the population can be trapped in the probe atom, indicating that at these distances there are no radiative modes available for emission. This is a situation similar to what one encounters in a Fabry-Pérot cavity composed of a pair of parallel-plate mirrors [39].

Polar diagrams have been presented showing the variation of the directivity function of the time-dependent as well as the stationary fields with various separations between atoms. We have found that the directional properties of the radiation field are generally more clearly manifested in the stationary field when the probe atom is continuously driven by a coherent laser field.

The control of directionality of photon emission could have promising applications in quantum information processing in realizing a directional quantum network. For example, the strong focusing of the radiation along the interatomic axis and the mirrorlike behavior reported here would be of great interest in the realization of a one-dimensional quantum network [4,5,9]. It could also be used as an optical reflector or an optical mirror to create, together with a distant dielectric mirror, a Fabry-Pérot cavity [14].

ACKNOWLEDGMENTS

Q.G. acknowledges support from the sixth research grant (Proposal No. 3775) funded by Jazan University, Saudi Arabia.

APPENDIX A: ATOMIC CORRELATION FUNCTIONS IN THE COLLECTIVE-STATE BASIS

The properties of the atomic correlation functions can be studied in terms of the density matrix elements of the operator ρ written in the basis of the free Hamiltonian H_0 excluding the contribution of the driving field. In the absence of the driving field ($\Omega_0 = 0$) the eigenstates of the free Hamiltonian H_0 and their energies are

$$\begin{aligned}
|1\rangle &= |g_1\rangle|g_2\rangle|g_3\rangle, \quad E_1 = 0,\\
|2\rangle &= |g_1\rangle|g_2\rangle|e_3\rangle, \quad E_2 = \hbar\omega_0,\\
|3\rangle &= |g_1\rangle|e_2\rangle|g_3\rangle, \quad E_3 = \hbar\omega_0,\\
|4\rangle &= |e_1\rangle|g_2\rangle|g_3\rangle, \quad E_4 = \hbar\omega_0,\\
|5\rangle &= |g_1\rangle|e_2\rangle|e_3\rangle, \quad E_5 = 2\hbar\omega_0,\\
|6\rangle &= |e_1\rangle|g_2\rangle|e_3\rangle, \quad E_6 = 2\hbar\omega_0,\\
|7\rangle &= |e_1\rangle|e_2\rangle|g_3\rangle, \quad E_7 = 2\hbar\omega_0,\\
|8\rangle &= |e_1\rangle|e_2\rangle|e_3\rangle, \quad E_8 = 3\hbar\omega_0. \qquad \text{(A1)}
\end{aligned}$$

The natural treatment for interacting atoms is the analysis in the basis of the eigenstates of the Hamiltonian $H_0 + H_{dd}$, the so-called collective states, which can be expressed in terms of the bare atomic states. The Hamiltonian $H_0 + H_{dd} \equiv \tilde{H}$

written in the basis of states (A1) has a matrix form,

$$\tilde{H} = \hbar \begin{pmatrix} 0 & 0 & 0 & 0 \\ 0 & \omega_0 I + M_1 & 0 & 0 \\ 0 & 0 & 2\omega_0 I + M_2 & 0 \\ 0 & 0 & 0 & 3\omega_0 \end{pmatrix}, \quad \text{(A2)}$$

where

$$M_1 = \begin{pmatrix} 0 & \Omega_{23} & \Omega_{13} \\ \Omega_{23} & 0 & \Omega_{12} \\ \Omega_{13} & \Omega_{12} & 0 \end{pmatrix}, \quad M_2 = \begin{pmatrix} 0 & \Omega_{12} & \Omega_{13} \\ \Omega_{12} & 0 & \Omega_{23} \\ \Omega_{13} & \Omega_{23} & 0 \end{pmatrix}, \quad \text{(A3)}$$

and I is the 3×3 unit matrix. Matrix (A3) is block diagonal, composed of two one-dimensional blocks and two 3×3 blocks, M_1 and M_2. Thus, the diagonalization of the 8×8 matrix, (A3), reduces to a diagonalization of matrices M_1 and M_2. In fact, it is enough to diagonalize matrix M_1. The eigenvalues and eigenvectors of matrix M_2 are then obtained by replacing $\omega_0 \to 2\omega_0$ and interchanging $\Omega_{12} \leftrightarrow \Omega_{23}$.

Since Ω_{ij} is significant for atomic separations $r_{ij} \leqslant \lambda/4$, we have that at distances $r_{13} > \lambda/2$ we can put $\Omega_{13} = 0$ in matrices M_1 and M_2. In this case, a substantial simplification arises in the diagonalization of the matrix $\omega_0 I + M_1$, leading to the eigenvalues

$$z_2 = \omega_0, \quad z_3 = \omega_0 + \Omega, \quad z_4 = \omega_0 - \Omega, \quad \text{(A4)}$$

where $\Omega = \sqrt{\Omega_{12}^2 + \Omega_{23}^2}$.

For the eigenvalue z_2, the corresponding eigenstate is

$$|\Psi_2\rangle = -\sin\varphi|2\rangle + \cos\varphi|4\rangle, \quad \text{(A5)}$$

where $\sin\varphi = \Omega_{12}/\Omega$ and $\cos\varphi = \Omega_{23}/\Omega$. For the eigenvalues z_3 and z_4 the corresponding eigenstates are

$$|\Psi_3\rangle = \frac{1}{\sqrt{2}}(|s\rangle + |3\rangle), \quad z_3 = \omega_0 + \Omega,$$
$$|\Psi_4\rangle = \frac{1}{\sqrt{2}}(-|s\rangle + |3\rangle), \quad z_4 = \omega_0 - \Omega, \quad \text{(A6)}$$

where

$$|s\rangle = \cos\varphi|2\rangle + \sin\varphi|4\rangle. \quad \text{(A7)}$$

The eigenvalues and eigenvectors of matrix M_2 are obtained by replacing $\omega_0 \to 2\omega_0$ and interchanging $\Omega_{12} \leftrightarrow \Omega_{23}$ in Eqs. (A4)–(A6). Hence, the eigenstates of matrix M_2 and the corresponding energies are

$$|\Psi_5\rangle = -\cos\varphi|5\rangle + \sin\varphi|7\rangle, \quad z_5 = 2\omega_0,$$
$$|\Psi_6\rangle = \frac{1}{\sqrt{2}}(|s'\rangle + |6\rangle), \quad z_6 = 2\omega_0 + \Omega, \quad \text{(A8)}$$
$$|\Psi_7\rangle = \frac{1}{\sqrt{2}}(-|s'\rangle + |6\rangle), \quad z_7 = 2\omega_0 - \Omega,$$

where

$$|s'\rangle = \sin\varphi|5\rangle + \cos\varphi|7\rangle. \quad \text{(A9)}$$

Having the collective states available, call them $|\Psi_1\rangle, |\Psi_2\rangle, \ldots |\Psi_8\rangle$, we can express the atomic correlation functions $\langle S_i^+ S_j^-\rangle$ in terms of the density matrix elements in the basis of the $|\Psi_i\rangle$ states. For example,

$$\langle S_1^+ S_2^-\rangle = \mathrm{Tr}\{S_1^+ S_2^- \rho\} = \mathrm{Tr}\left\{\sum_{i,j=1}^{8} \rho_{ij} S_1^+ S_2^- |\Psi_i\rangle\langle\Psi_j|\right\}. \quad \text{(A10)}$$

Thus, it requires calculation of the result of $S_1^+ S_2^- |\Psi_i\rangle$ before application of the trace. The required products of the atomic operators are

$$\begin{aligned} S_1^+ S_1^- + S_2^+ S_2^- + S_3^+ S_3^- &= 3|8\rangle\langle 8| + 2|7\rangle\langle 7| + 2|6\rangle\langle 6| \\ &\quad + 2|5\rangle\langle 5| + |4\rangle\langle 4| + |3\rangle\langle 3| + |2\rangle\langle 2|, \\ S_1^+ S_2^- + S_2^+ S_1^- &= |6\rangle\langle 5| + |5\rangle\langle 6| + |4\rangle\langle 3| + |3\rangle\langle 4|, \\ S_1^+ S_2^- - S_2^+ S_1^- &= |6\rangle\langle 5| - |5\rangle\langle 6| + |4\rangle\langle 3| - |3\rangle\langle 4|. \end{aligned} \quad \text{(A11)}$$

We express the bare atomic states in terms of two independent sets of collective states,

$$\begin{aligned} |1\rangle &= |\Psi_1\rangle, \\ |2\rangle &= -\sin\varphi|\Psi_2\rangle + \frac{\cos\varphi}{\sqrt{2}}(|\Psi_3\rangle - |\Psi_4\rangle), \\ |3\rangle &= \frac{1}{\sqrt{2}}(|\Psi_3\rangle + |\Psi_4\rangle), \\ |4\rangle &= \cos\varphi|\Psi_2\rangle + \frac{\sin\varphi}{\sqrt{2}}(|\Psi_3\rangle - |\Psi_4\rangle) \end{aligned} \quad \text{(A12)}$$

and

$$\begin{aligned} |5\rangle &= -\cos\varphi|\Psi_5\rangle + \frac{\sin\varphi}{\sqrt{2}}(|\Psi_6\rangle - |\Psi_7\rangle), \\ |6\rangle &= \frac{1}{\sqrt{2}}(|\Psi_6\rangle + |\Psi_7\rangle), \\ |7\rangle &= \sin\varphi|\Psi_5\rangle + \frac{\cos\varphi}{\sqrt{2}}(|\Psi_6\rangle - |\Psi_7\rangle), \\ |8\rangle &= |\Psi_8\rangle. \end{aligned} \quad \text{(A13)}$$

Hence

$$\begin{aligned} S_1^+ S_1^- + S_2^+ S_2^- &= P_{22}\cos^2\varphi + \frac{1}{2}(1 + \sin^2\varphi)(P_{33} + P_{44}) \\ &\quad + \mathrm{Re}\left[P_{34}\cos^2\varphi + \frac{\sin 2\varphi}{\sqrt{2}}(P_{23} - P_{24})\right], \\ S_1^+ S_2^- + S_2^+ S_1^- &= (P_{33} - P_{44} + P_{66} - P_{77})\sin\varphi \\ &\quad + \sqrt{2}\,\mathrm{Re}[P_{23} + P_{24} - P_{56} - P_{57}]\cos\varphi, \\ S_1^+ S_2^- - S_2^+ S_1^- &= 2\,\mathrm{Im}[P_{43} + P_{76}]\sin\varphi + \sqrt{2}\,\mathrm{Im}[P_{56} + P_{57} \\ &\quad + P_{32} + P_{42}]\cos\varphi, \end{aligned} \quad \text{(A14)}$$

where $P_{ij} = |\Psi_i\rangle\langle\Psi_j|$.

It is clearly seen from Eq. (A14) that the real parts of the atomic correlation functions depend on the populations of the collective states and coherences between them, while the imaginary parts depend solely on the coherences. Thus, crucial for the imaginary parts of the atomic correlation functions to be nonzero is to prepare or drive the atomic system such that there are nonzero coherences between the collective states.

APPENDIX B: EQUATIONS OF MOTION FOR THE DENSITY MATRIX ELEMENTS

Assuming that only one atom at the most can be excited at any time t, the time-dependent state vector can be written as

$$|\psi(t)\rangle = \sum_{i=1}^{N} b_i(t)|i\rangle + b_{N+1}(t)|N+1\rangle, \tag{B1}$$

where the ket vector $|i\rangle$ represents the combined state of the N atoms, respectively, with only the ith atom excited. $|N+1\rangle$ represents the collective ground state of all N atoms with no atom excited.

Using the master equation, (1), it is straightforward to show that the density matrix elements obey the set of equations

$$\dot{\rho}_{l,l}(t) = \frac{d}{dt}|b_l(t)|^2 = -\gamma|b_l(t)|^2 - \sum_{j\neq l}\left\{\left[i\Omega^{(lj)} + \frac{\gamma^{(lj)}}{2}\right]b_j^*(t)b_l(t) + \text{H.c.}\right\}, \tag{B2a}$$

$$\dot{\rho}_{N+1,N+1}(t) = \frac{d}{dt}|b_{N+1}(t)|^2 = \gamma\sum_{j=1}^{N}|b_j(t)|^2 + \frac{1}{2}\sum_{i=1}^{N}\sum_{j=i+1}^{N}\{[\gamma^{(ij)} + \gamma^{(ji)}](b_i^*(t)b_j(t) + \text{H.c.})\}, \tag{B2b}$$

$$\begin{aligned}\dot{\rho}_{m,n}(t)\Big|_{\substack{\{m,n\}\in\{1,\ldots,N\}\\ m\neq n}} &= \frac{d}{dt}[b_m^*(t)b_n(t)] \\ &= -\gamma b_m^*(t)b_n(t) - \sum_{\substack{j=1\\ j\neq m}}^{N}\left[i\Omega^{(mj)} + \frac{1}{2}\gamma^{(mj)}\right]b_j^*(t)b_n(t) + \sum_{\substack{j=1\\ j\neq n}}^{N}\left[i\Omega^{(nj)} - \frac{\gamma^{(nj)}}{2}\right]b_m^*(t)b_j(t),\end{aligned} \tag{B2c}$$

$$\dot{\rho}_{l,N+1}(t) = -\sum_{\substack{j=1\\ j\neq l}}^{N}\left[i\Omega^{(lj)} + \frac{\gamma^{(lj)}}{2}\right]b_j^*(t)b_{N+1}(t) - \frac{1}{2}\gamma b_l^*(t)b_{N+1}(t), \tag{B2d}$$

where $\{l,m,n\} \in \{1,\ldots,N\}$. The remaining equations for the off-diagonal matrix elements can be obtained from Eqs. (B2c) and (B2d) by complex conjugation. We see that throughout Eqs. (B2a)–(B2d), sums over different atoms appear repeatedly, providing the source of coupling between different atoms.

[1] I. Bloch, J. Dalibard, and W. Zwerger, Rev. Mod. Phys. **80**, 885 (2008).
[2] M. Saffman, T. G. Walker, and K. Molmer, Rev. Mod. Phys. **82**, 2313 (2010).
[3] D. Comparat and P. Pillet, J. Opt. Soc. Am. B **27**, A208 (2010).
[4] K. P. Nayak, P. N. Melentiev, M. Morinaga, F. Le Kien, V. I. Balykin, and K. Hakuta, Opt. Express **15**, 5431 (2007).
[5] E. Vetsch, D. Reitz, G. Sagué, R. Schmidt, S. T. Dawkins, and A. Rauschenbeutel, Phys. Rev. Lett. **104**, 203603 (2010).
[6] X.-F. Qian, Y. Li, Y. Li, Z. Song, and C. P. Sun, Phys. Rev. A **72**, 062329 (2005).
[7] D. E. Chang, L. Jiang, A. V. Gorshkov, and H. J. Kimble, New J. Phys. **14**, 063003 (2012).
[8] D. E. Chang, J. I. Cirac, and H. J. Kimble, Phys. Rev. Lett. **110**, 113606 (2013).
[9] T. Shi, D. E. Chang, and J. I. Cirac, Phys. Rev. A **92**, 053834 (2015).
[10] H. Pichler, T. Ramos, A. J. Daley, and P. Zoller, Phys. Rev. A **91**, 042116 (2015).
[11] B. Vermersch, T. Ramos, P. Hauke, and P. Zoller, Phys. Rev. A **93**, 063830 (2016).
[12] P. Lodahl, S. Mahmoodian, S. Stobbe, P. Schneeweiss, J. Volz, A. Rauschenbeutel, H. Pichler, and P. Zoller, arXiv:1608.00446.
[13] C. Gonzalez-Ballestero, A. Gonzalez-Tudela, F. J. Garcia-Vidal, and E. Moreno, Phys. Rev. B **92**, 155304 (2015).
[14] G. Hétet, L. Slodicka, M. Hennrich, and R. Blatt, Phys. Rev. Lett. **107**, 133002 (2011).
[15] L. Zhou, H. Dong, Y.-x. Liu, C. P. Sun, and F. Nori, Phys. Rev. A **78**, 063827 (2008).
[16] P.-O. Guimond, A. Roulet, H. N. Le, and V. Scarani, Phys. Rev. A **93**, 023808 (2016).
[17] R. H. Dicke, Phys. Rev. **93**, 99 (1954).
[18] R. H. Lehmberg, Phys. Rev. A **2**, 889 (1970).
[19] Th. Richter, J. Phys. B: At. Mol. Phys. **15**, 1293 (1982).
[20] H. Blank, M. Blank, K. Blum, and A. Faridani, Phys. Lett. A **105**, 39 (1984).
[21] H. S. Freedhoff, J. Chem. Phys. **85**, 6110 (1986).
[22] Z. Ficek, R. Tanaś, and S. Kielich, Physica A **146**, 452 (1987).

[23] S. Das, G. S. Agarwal, and M. O. Scully, Phys. Rev. Lett. **101**, 153601 (2008).
[24] J. Eschner *et al.*, Nature **413**, 495 (2001); S. Rist, J. Eschner, M. Hennrich, and G. Morigi, Phys. Rev. A **78**, 013808 (2008).
[25] C. Hettich *et al.*, Science **298**, 385 (2002).
[26] J. P. Clemens, L. Horvath, B. C. Sanders, and H. J. Carmichael, Phys. Rev. A **68**, 023809 (2003).
[27] C. J. Mewton and Z. Ficek, J. Phys. B: At. Mol. Opt. Phys. **B40**, S181 (2007).
[28] D. Porras and J. I. Cirac, Phys. Rev. A **78**, 053816 (2008).
[29] R. Wiegner, J. von Zanthier, and G. S. Agarwal, Phys. Rev. A **84**, 023805 (2011).
[30] Z. Liao and M. S. Zubairy, Phys. Rev. A **90**, 053805 (2014).
[31] J. A. Mlynek, A. A. Abdumalikov, Jr., J. M. Fink, L. Steffen, M. Baur, C. Lang, A. F. van Loo, and A. Wallraff, Phys. Rev. A **86**, 053838 (2012).
[32] F. Nissen, J. M. Fink, J. A. Mlynek, A. Wallraff, and J. Keeling, Phys. Rev. Lett. **110**, 203602 (2013).
[33] A. F. van Loo, A. Fedorov, K. Lalumiere, B. C. Sanders, A. Blais, and A. Wallraff, Science **342**, 1494 (2013).
[34] G. S. Agarwal, *Springer Tracts in Modern Physics: Quantum Optics* (Springer-Verlag, Berlin, 1974).
[35] M. Kiffner, M. Macovei, J. Evers, and C. H. Keitel, in *Progress in Optics*, edited by E. Wolf (Elsevier, Amsterdam, 2010), Vol. 55.
[36] Z. Ficek and S. Swain, *Quantum Interference and Coherence: Theory and Experiments* (Springer, New York, 2005), Vol. 100.
[37] M. O. Scully and M. S. Zubairy, *Quantum Optics* (Cambridge University Press, Cambridge, UK, 1997).
[38] H. J. Kimble and L. Mandel, Phys. Rev. A **13**, 2123 (1976).
[39] J. P. Dowling, M. O. Scully, and F. DeMartini, Opt. Commun. **82**, 415 (1991).